ELSEVIER

Marine Geology 188 (2002) 351–364

MARINE GEOLOGY
INTERNATIONAL JOURNAL OF MARINE GEOLOGY, GEOCHEMISTRY AND GEOPHYSICS

www.elsevier.com/locate/margeo

Numerical simulation of mud-rich subaqueous debris flows on the glacially active margins of the Svalbard–Barents Sea

Jeffrey G. Marr [a,*], Anders Elverhøi [b], Carl Harbitz [c], Jasim Imran [d], Peter Harff [a]

[a] *St. Anthony Falls Laboratory, University of Minnesota, Mississippi River at 3rd Ave. SE, Minneapolis, MN 55414, USA*
[b] *Department of Geology, University of Oslo, P.O. Box 1047, Blindern, N-0316 Oslo, Norway*
[c] *Norwegian Geotechnical Institute, P.O. Box 3930, Ullevål Stadion, N-0806 Oslo, Norway*
[d] *Department of Civil and Environmental Engineering, University of South Carolina, Columbia, SC 29208, USA*

Received 18 March 2002; accepted 8 April 2002

Abstract

Seismic images and sediment core data from the Bear Island and Isfjorden fans localized along the Svalbard–Barents Sea continental margin, reveal an interesting depositional system consisting of stacked debris flow lobes. The frequent release of debris flows was associated with large volumes of sediment rapidly delivered to the shelf break during periods of maximum glaciation. The compositions of the lobes for both fans are similar, consisting of mainly clay and silt. The data show, however, a dramatic difference in runout distances for the two areas. Isfjorden debris lobes are 10–30 km in length whereas Bear Island lobes are 100–200 km in length. Even more intriguing is the fact that the large runout distances on the Bear Island fan occurred on slopes less than 1° whereas the Isfjorden fan flows occurred on slopes greater than 4°. Depth-averaged non-linear one-dimensional equations for balance of mass and linear momentum are applied to simulate the subaqueous debris flow. The equations are solved by the numerical model BING, describing the flow as a visco-plastic Bingham fluid. The model is employed to study the effect yield strength, viscosity and bathymetry have on debris flow runout. The study shows that the large runout distances can be achieved on the Bear Island fan by visco-plastic flows with sufficiently low yield strength. High yield strength sediments require an additional mechanism, such as hydroplaning, to reach measured runout distances. Most importantly, this study shows the necessity of good rheological measurements for accurate numerical modeling of subaqueous debris flows.

Keywords: debris flow; gravity flow; hydroplaning; modelling; rheology; submarine

1. Introduction

Subaqueous debris flows play a major role in the movement of sediment from the continental shelf and upper slope to the deep ocean. Such flows have implications on the long-term environmental or basin systems as well as a more immediate and direct impact on human life. Debris flows along with turbidity currents are instrumental in the formation of subaqueous fans (Prior and Bornhold, 1986; Laberg and Vorren, 1993;

* Corresponding author. Tel.: +1-612-627-4602; Fax: +1-612-627-4609.
E-mail address: marrx003@ umn.edu (J.G. Marr).

0025-3227/02/$ – see front matter
PII: S0025-3227(02)00310-9

Piper et al., 1997). Understanding the flow dynamic as well as the range of potential deposit geometries resulting from these flows aid in the interpretation of depositional systems. Modern debris flows impose risk to marine structures such as platforms, pipelines, and cables (Heezen and Ewing, 1952; Krause et al., 1970; Bea, 1971; Bjerrum, 1971; Hampton et al., 1996). Tsunami generation from subaqueous debris flows is also a risk to offshore constructions and coastal communities (Murty, 1979; Moore and Moore, 1984, 1988; Harbitz, 1992; Kulikov et al., 1996). Back-analysis of tsunamis in combination with tide gauge or deep-sea pressure sensor records can provide valuable information regarding the initial location, extent (volume), shape and motion of the tsunami source. An overview of registered submarine slide events is given by Moore (1978), Lee (1989), and Hampton et al. (1996).

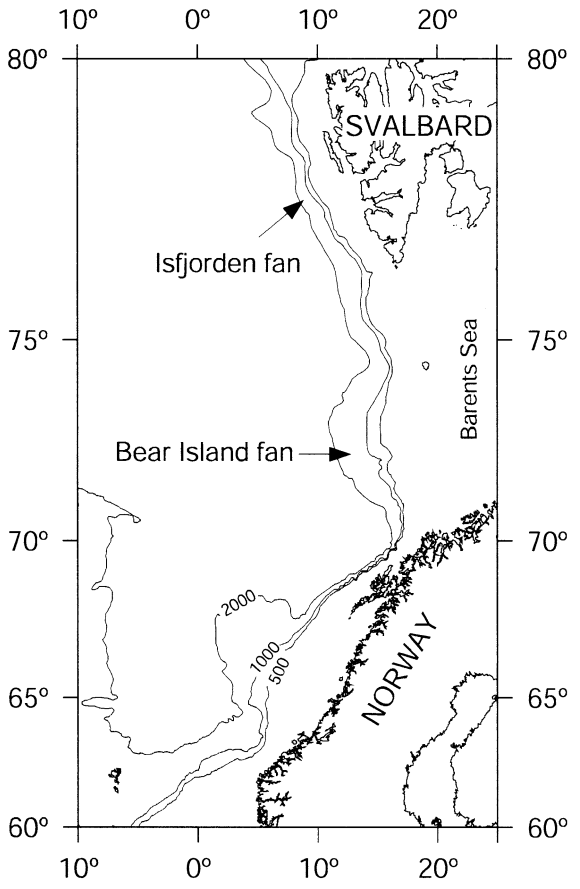

Fig. 1. Location of the study areas: Isfjorden fan and Bear Island fan.

The Bear Island and Isfjorden fans, located along the Svalbard–Barents Sea continental margin (Fig. 1) are dominated by debris flow deposition. Both systems are thought to have been geologically active during periods of glaciation. Over relatively short periods (i.e. 3000–5000 yr) sediment was delivered to the shelf-slope break as a deformation till under glacial ice (Fig. 2) resulting in high rates of sedimentation (0.6 m y^{-1}) at the slope-break (Laberg and Vorren, 1995; Elverhøi et al., 1997; Dowdeswell and Siegert, 1999). Dimakis et al. (2000) estimated that the high sedimentation rates in these areas resulted in build-up of excess pore-pressure leading to subsequent failure of sediment. The submarine debris flow deposits in question are attributed to failure of these sediments.

The main motivation for this study comes out of observed differences in debris flow runout distances on the Isfjorden and Bear Island fans. The Isfjorden fan has debris flow runout distances ranging from 10 to 30 km whereas the Bear Island fan deposits have runout distances ranging from 100 to 200 km (Elverhøi et al., 1997). A relatively steep slope (3–4°) characterizes the Isfjorden fan while the Bear Island fan has a measured slope of 0.2–0.5° (Laberg and Vorren, 1995).

The sediment comprising the debris flows in both regions is similar (Table 1). The debris flow sediment on the Isfjorden fan is comprised of 35–40 wt% clay, 35–40 wt% silt and 20–30 wt% sand (Elverhøi et al., 1997). Sediment from the Bear Island fan is reported to be 30–55 wt% clay, 30–50 wt% silt, 10–30 wt% sand and 1–10 wt% gravel (Laberg and Vorren, 1995). In both regions, over 75 wt% of the sediment is clay and silt.

2. Approach

The differences in the runout distances of the observed deposits can be explained in terms of either the *release volume*, the *rheological properties* of the sediment, or the *flow mechanics* of the debris.

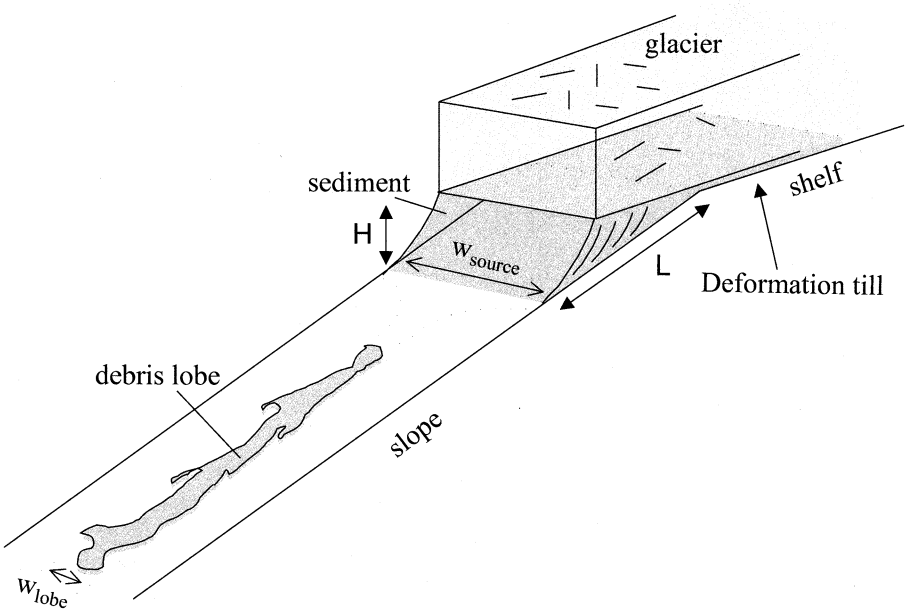

Fig. 2. Conceptual model illustrating the primary sediment delivery mechanism during maximum glaciation for the study areas. The width of the final deposit lobe is much smaller than the width of the source area, indicating restriction or funneling of the flow ($w_{source} > w_{lobe}$).

The amount of material mobilized in a failure or *release volume* influences runout distance. Larger amounts of material result in longer runout distances. This behavior has been observed for subaqueous debris flows (Edgers and Karlsrud, 1982), subaerial debris flows (Iverson, 1997), rockslides (Heim, 1932; Scheidegger, 1973), and snow avalanches (Salm et al., 1990; McClung and Schaerer, 1993; Harbitz et al., 1998). Several similarities between subaqueous gravity mass flows and snow avalanches indicate that experimental and theoretical experience from snow avalanches can be transferred into the study of subaqueous mass flows (Norem et al., 1990). Hence, it is worth noting that snow avalanche studies reveal that lower slope environments normally permit more snow to be accumulated before release, resulting in larger and less frequent events (Lied and Bakkehøi, 1980). This suggests that failures on the Bear Island fan, with a slope of $< 0.5°$, may have been larger than failures on the Isfjorden fan resulting in longer runout distances. *Rheological properties* are determined by fines content, clay mineralogy, coarse-grain composition and distribution and water content (Middleton and Hampton, 1973; Coussot, 1997). The rheological properties of a failed mass of sediment determines the response of the sediment to external and internal forces such as bed friction, surface stress, internal shear, and gravity.

Table 1
Sediment and environmental properties of the Isfjorden and Bear Island fans[a]

Fan	Isfjorden	Bear Island
Runout distance (km)	10–30	100–200
Width (km)	1–5	5–25
Thickness (m)	10–30	10–50
Volume (km^3)	0.5–1	10–30
Slope angle (°)[c]	3–4	0.2–0.5
Grain size (μm,%)	< 2, 35–40%	< 2, 30–55%
	2–63, 35–40%	2–63, 30–50%
	> 63, 20–30%	> 63, 10–30%
Bulk density (kg/m^3)	2000	1800
Yield strength (kPa)[b]	10–25	1–5/10–25

[a] Data were compiled from the following sources: Laberg and Vorren (1993, 1995) and Elverhøi et al. (1997).

[b] Bear Island simulation included two ranges of yield strength as listed.

[c] Slope angle is average angle of entire fan surface.

A difference in the *flow mechanics* of the debris flows in the two study areas is another possible explanation for the observed variations in runout distances. Recent laboratory experiments on small-scale, subaqueous debris flows suggest that hydroplaning is an alternative mechanism for extending the runout distances of debris flows (Mohrig et al., 1998, 1999). Hydroplaning in subaqueous debris flows occurs when a thin layer of water becomes trapped under the leading edge of a sediment flow, thereby reducing the friction at the bed and potentially increasing both head velocity and runout distance. Because the trapped water takes on most of the shear of the flow, the flow mechanics of hydroplaning sediment is decoupled from sediment rheology (Harbitz et al., in review). In this way the Bear Island fan sediment could be of the same rheology as on the Isfjorden and still reach longer runout distances.

The numerical model BING is used to investigate the influence of failure volume, sediment rheology, and flow mechanics on runout distance for sediment observed on the Bear Island and Isfjorden fans. As will be explained in more detail below, the sediment is assumed to follow a simple Bingham rheology. Field data are used in conjunction with numerical results to gain insight into the natural systems.

3. Bingham rheology

The mechanics of both subaerial and subaqueous debris flows are complex, involving properties similar to those employed in fluid, particle, and soil mechanics. Frictional interaction between grains, viscous and cohesional behavior of clays, and collisional dampening by pore-water all factor into the transfer of momentum within a debris flow (Hampton, 1975; Coussot, 1997; Iverson, 1997; Whipple, 1997). Modeling such a system particle-by-particle quickly becomes computationally cumbersome. As an alternative, several simplified rheological models are commonly used to approximate the flow behavior of debris flows. The Herschel–Bulkley and Bingham models are the most common for muddy debris flows.

The constitutive equation for the Herschel–Bulkley model is as follows:

$$\tau = \tau_y + K\left(\frac{\partial u}{\partial y}\right)^n \quad (1)$$

where τ, τ_y, K, and $\partial u/\partial y$ represent the shear stress, yield strength, 'viscosity', and shear rate, respectively. The exponent n is adjusted to fit measured data (Huang and García, 1998). When the exponent $n \rightarrow 1$, $K \rightarrow \mu$ where μ represents the dynamic viscosity of the sediment. In this case Eq. 1 takes the form of the constitutive equation for a Bingham fluid. Fig. 3 shows the stress/strain relationship for an ideal Bingham fluid. The model requires that motion of the fluid does not begin until the yield strength of the fluid is exceeded, after which the fluid flows as a Newtonian fluid with a linear stress/strain rate relationship determined by the dynamic viscosity of the fluid. The yield strength and the viscosity are characteristics of the sediment. Bingham rheology assumes that the behavior of the whole thickness of the flow is governed by the shearing behavior of the matrix or fine material (clay and silt) in the debris flow. Most importantly, collisional/frictional interactions between grains are assumed negligible, i.e. energy dissipation is caused by viscosity of the matrix fluid between particles. As described by Bagnold (1954, 1956), this gives rise to a dynamic shear (not included in the Herschel–Bulkley or

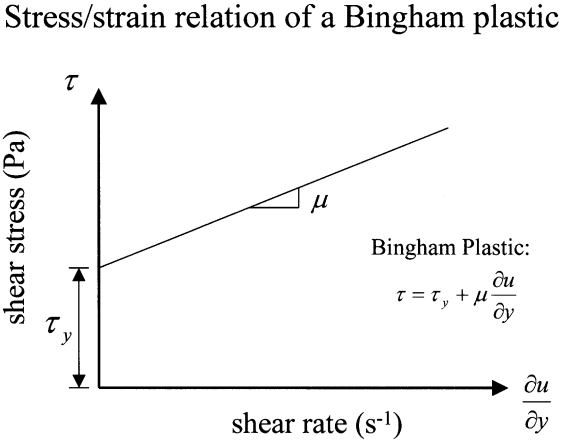

Fig. 3. Stress/strain relationship for an ideal Bingham plastic.

Bingham models), and a dispersive pressure normal to the flow direction, which reduces the internal friction. The latter is caused by the influence of the grains on the flow patterns of the fluid around neighboring grains. The simulations presented in this paper utilize a Bingham rheology ($n = 1$).

The application of Bingham rheology to sediment gravity flows has been challenged (Norem et al., 1990; Iverson, 1997; Huang and García, 1998, 1999). The model falls short mainly in the case of coarse-grained debris flows. The simple constitutive relationship of Eq. 1 is not able to capture the complicated grain–grain and grain–water interactions controlling these flows. More comprehensive models are required in these cases (Takahashi, 1978; Norem et al., 1990; Iverson, 1997; Huang and García, 1998).

Large-scale measurements of sediment rheology have shown that the Bingham model is applicable for some debris flows. O'Brien and Julien (1988) tested natural subaerial debris flow material in a rotary viscometer. They were able to successfully apply the Bingham model to mud-rich mixtures (i.e. sand volumetric concentrations $< 20\%$). Experiments by Phillips and Davies (1990) were performed using a large (2 m) inverted cone rheometer. They concluded that debris flow material with high fines content or low content of coarse material followed a visco-plastic rheology. Similar experiments by Major and Pierson (1992) performed in a specially constructed concentric-circle viscometer also showed that fine-grained sediment mixtures followed a Bingham-type rheology.

The sediment comprising the subaqueous debris flow lobes of the Bear Island and Isfjorden fans is composed primarily of silt and clay with some sand. Based on the experimental findings discussed above we assume that the subaqueous debris flows found in the study areas flowed as Bingham fluids rather than frictional debris flows often encountered in coarser-granular flows.

4. Numerical simulation

We use the numerical code BING to explore the relationship between failure volume, sediment rheology, longitudinal path profile (bathymetry), runout distance, and deposit thickness. The numerical model BING developed by Imran et al. (2001) uses Herschel–Bulkley (Johnson, 1970; Huang and García, 1999) and bilinear rheologies (Locat, 1997). The model is based on the numerical model of Jiang and LeBlond (1993). As described earlier, the Bingham rheology considered in the present work is a limiting case of the Herschel–Bulkley rheology and is not treated separately in BING. The numerical model solves conservation of mass and momentum equations that are integrated over the viscous and the plug layer thicknesses and then expressed in a Lagrangian framework. The Lagrangian form reduces the mass conservation equation into a kinematic equation, and combines the local and convective acceleration into a total derivative in the momentum equations. The momentum equations are solved using an explicit finite difference scheme. The number of grid cells remains the same throughout the calculation. Each grid node is allowed to move at the local depth-averaged velocity after each time step. As a result neighboring nodes can move closer or away from each other. Starting from an initial parabolic shape the debris mass is allowed to stretch until the front velocity decelerates to a negligible value at which point the calculation is terminated. The model enforces a no-slip bed condition and erosion, deposition, and entrainment of water are neglected. The reader is referred to Imran et al. (2001) for details of the numerical model.

Determination of the values of the input parameters for the model are made from previous work on the study areas (Laberg and Vorren, 1995; Elverhøi et al., 1997; Dimakis et al., 2000). Table 2 lists the input parameter values used in the BING simulations for both the Isfjorden and Bear Island fans. Special attention is placed on determining longitudinal path profile, sediment properties, and failure geometry.

Longitudinal path profiles obtained from seismic surveys and bathymetric maps of the study areas are used in the model simulation. The slope on the Isfjorden fan ranges from 3 to 4° while the slope of the Bear Island fan ranges from 0.2 to 0.5° (Fig. 4).

Table 2
Input parameter values used in BING simulations

Fan	Isfjorden Case 1	Bear Island Case 2	Bear Island Case 3
Failure geometry			
Volume/unit width (km^2)	0.4	3	3
Length of deposit (km)	6.67	20	20
Thickness of deposit (m)	90	225	225
Sediment properties			
Viscosity (Pa s)	300, 30	300, 30	300, 30
Yield strength (kPa)	10–25	1–5	10–25
Bulk density (kg/m^3)	2000	1800	1800

Sediment properties reflecting the sediment rheology are the most important parameters of the model and the most difficult to determine. They influence the model output significantly. The parameters required are sediment bulk density, yield strength, and dynamic viscosity.

1. Bulk density, ρ_s, is determined through laboratory measurements. The sediment from the North Sea has a bulk density ranging from 1800 to 2000 kg/m^3.

2. Yield strength, τ_y, of the slurry represents the stress at which a static Bingham material begins motion. Yield strengths for typical debris flow material spans the range 10^1 to 10^5 Pa (Major and Pierson, 1992; Coussot, 1997; Locat, 1997; Whipple, 1997). Determination of yield strength can be made through a laboratory test of sediment in a rheometer. It can also be determined by analysis of the deposit. Johnson (1970) suggested that termination of flow of a Bingham fluid occurs when the driving stress drops below the yield strength of the sediment. Therefore the thickness of the final deposit may be used to characterize the yield strength. Eq. 2 describes this relationship for submerged sediment:

$$\tau_y = (\rho_s - \rho_w) g H \sin \alpha_d \quad (2)$$

where ρ_w, g, H, and α_d represent the density of water, acceleration of gravity, critical thickness of sediment, and the angle of the bed slope in the depositional area, respectively. By knowing the final thickness of the deposit (obtained from a seismic survey), the bed slope, and material densities, we can estimate the yield strength of the sediments.

Eq. 2 is effective with non-hydroplaning subaqueous debris flows or with subaerial debris

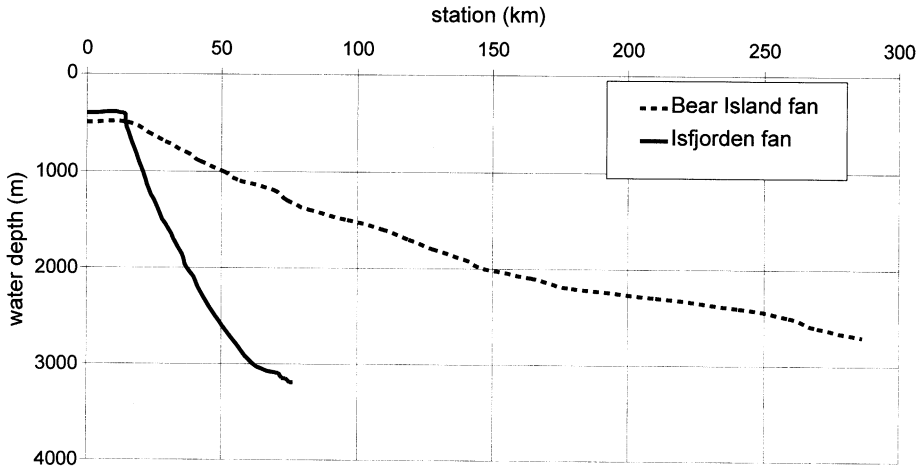

Fig. 4. Bathymetry of the Isfjorden and Bear Island fans used in the model simulations.

flows by removing the buoyancy correction term ($-\rho_w$), but fails in the case of subaqueous debris flows that hydroplane. The flow mechanics of hydroplaning debris flows no longer follow the simple Bingham model (Mohrig et al., 1998, 1999; Harbitz et al., in review). Laboratory observations of hydroplaning debris flows suggest that the acceleration of the downslope sediment (i.e. hydroplaning head) results in the extension of the main body of sediment yielding a thinner deposit than would result through normal Bingham flow (Mohrig et al., 1999; Huang and García, 1999). For this reason we need an alternative method to estimate the yield strength of debris flows that hydroplane.

The Isfjorden fan debris lobes (Case 1) are assumed to not have hydroplaned due to their relatively short runout distances. It is possible, however, that the long debris lobes of the Bear Island fan did hydroplane. For this reason two analyses are considered for the Bear Island fan: (Case 2) the non-hydroplaning case with yield strength estimated from Eq. 2; (Case 3) the hydroplaning case with yield strength assumed to be of the same order of magnitude as the Isfjorden fan sediments. The values used are listed in Table 2.

3. Dynamic viscosity coefficient, μ, of the field sediment was not possible to measure. For this reason we consider a range of dynamic viscosities from 30 to 300 Pa s based on reported measurements of viscosity from similar clay and silt rich sediments (Phillips and Davies, 1990; Major and Pierson, 1992; Coussot, 1997).

The *failure volume and geometry* are estimated based on the assumption that debris lobe volume correlates with release volume. Estimates of lobe volumes from the study sites are listed in Table 1 (Laberg and Vorren, 1995; Elverhøi et al., 1997). In order to use the estimates in the one-dimensional BING model, lobe volumes (km^3) are converted to volume per unit width, v, (km^2) by dividing by measured lobe width. These are listed in Table 2. BING approximates the geometry of the failed sediment as a parabola. The user specifies the most upstream point of the sediment, the length of the failed sediment, L, and the thickness of the sediment, H. The dimensions of the parabola are set so that the desired volume per unit width is modelled. Eq. 3 gives the relationship for the volume per unit width (equal to the area under the parabola) as a function of L and H.

$$v = \frac{2}{3}(L \times H) \tag{3}$$

However, sediment most likely failed near the shelf-slope break and funnelled into a narrow region of high gradient between pre-existing lobes. Hence, in the natural case (Fig. 2) the failure geometry was presumably wider and thicker than the final lobe. As a consequence of working in one horizontal dimension, the initial magnitude of L and H must therefore be larger than what is realistic to run the simulations with a correct volume. For example, given a failure volume per unit width, v, of 3 km^2 and a thickness, H, of 60 m (typical for the Bear Island Fan) Eq. 3 requires an L of 75 km. An extensive sensitivity analysis of the effects L, H, and v have on runout was performed, from which the most stable values of L and H were selected for the BING simulations.

5. Results

Three cases are simulated using BING. In Case 1 we examine the flow of the Isfjorden fan sediment assuming that the debris flows were viscoplastic, non-hydroplaning flows (yield strength estimated from field-measured thicknesses and Eq. 2). In Case 2 we consider the flow of Bear Island fan sediment with the same assumptions and estimates as in Case 1. Finally, in Case 3 we simulate the flow of Bear Island fan sediment with yield strength similar to the Isfjorden fan sediment.

5.1. Case 1 – Isfjorden fan simulation

Fig. 5 shows the runout and deposit thickness as a function of variable yield strength from eight simulations of subaqueous debris flows on the Isfjorden fan. Four yield strengths were considered in the range 10–25 kPa. For each yield strength viscosities of 30 and 300 Pa s were examined. A volume per unit width of 0.4 km^2 was

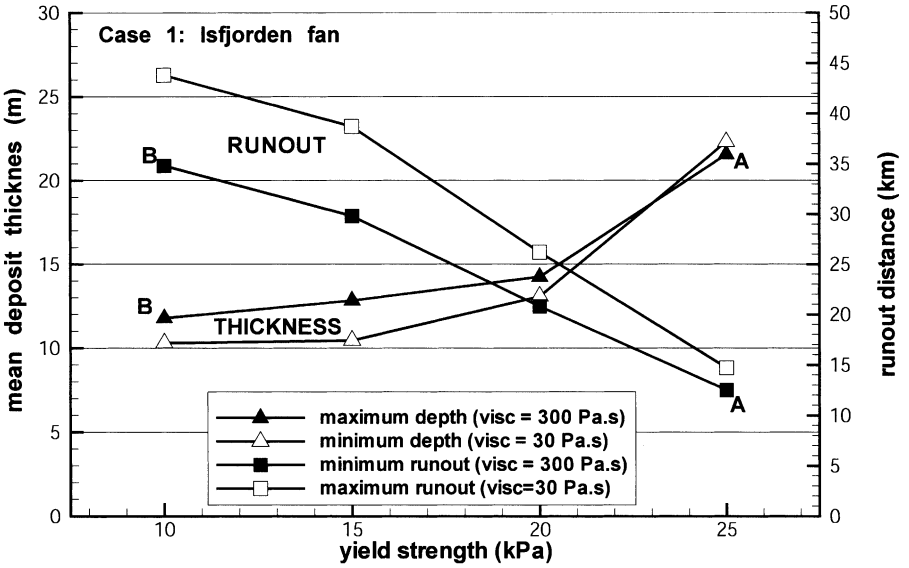

Fig. 5. Data plots from Case 1 simulations of the sediment flows on the Isfjorden fan showing sediment runout and depth as a function of sediment yield. For each yield strength two viscosities were considered. The runout distances are read on the right vertical axis and the deposit depths are read on the left vertical axis.

simulated for all runs. The largest runout distances and thinnest deposits were observed at the lowest yield strengths. Dynamic viscosity played a minor role in deposit thickness and only affected runout distance at the lowest yield strength, as represented by the large span of runout distances predicted by BING at 10 kPa. Fig. 6 shows the elevation distribution of the deposits for the case of 25 kPa (A) and the case of 10 kPa (B) both with viscosity of 300 Pa s.

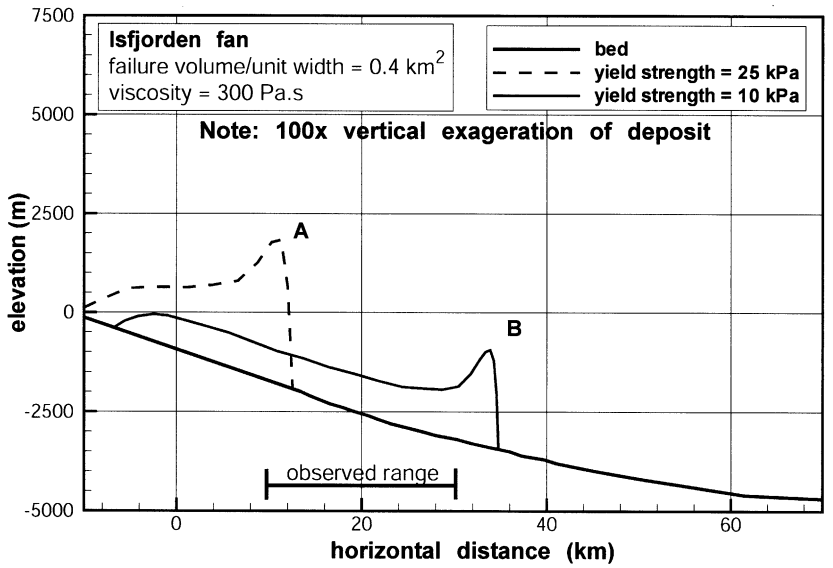

Fig. 6. Comparison plot of final deposit geometry of two simulations on the Isfjorden fan. A and B correlate to the A and B listed in Fig. 5.

Table 3
Model/field comparisons

Fan	Isfjorden Case 1	Bear Island Case 2 (small τ_y)	Bear Island Case 3 ($\tau_y \approx$ Isfjorden Fan)
Runout distance (km)			
Observed	10–30	100–200	100–200
BING simulation	13–44	77–355	7–35
Mean thickness (m)			
Observed	10–30	10–50	10–50
BING simulation	10–22	8–30	50–130

The BING simulations match the observed lobe geometry fairly well. Table 3 compares the results of the simulations with those observed from the actual deposits. At the yield strengths and viscosities examined, BING predicts runout distances ranging from 13 to 44 km, which agrees with the 10–30 km distances reported by Elverhøi et al. (1997). The final deposit thicknesses (10–22 m) also compare well with the 10–30 m range specified in the reported data. It is not surprising that the model results match those measured in the field since we used yield strength values that were calculated from observed deposit thickness and assumed the material flowed as a Bingham plastic. These results verify that the Bingham rheology and the BING model are able to replicate field observations.

5.2. Case 2 – Bear Island fan simulation: visco-plastic, Bear Island rheology

In this case we assume the debris flows on the Bear Island fan were formed purely by Bingham fluid behavior, that is without hydroplaning. Eq. 2 is used to determine the range of yield strength for the sediment, which is listed in Table 2. Simulations were run using this range as well as a volume per unit width of sediment of 3 km^2. The mean deposit thickness and runout predicted by BING are presented in Fig. 7. The same trend is observed for yield strength as was in Case 1: runout distance decreases and deposit thickness increases with increasing yield strength. Sediment with a lower viscosity travels farther than sediment with higher viscosity. This effect is more

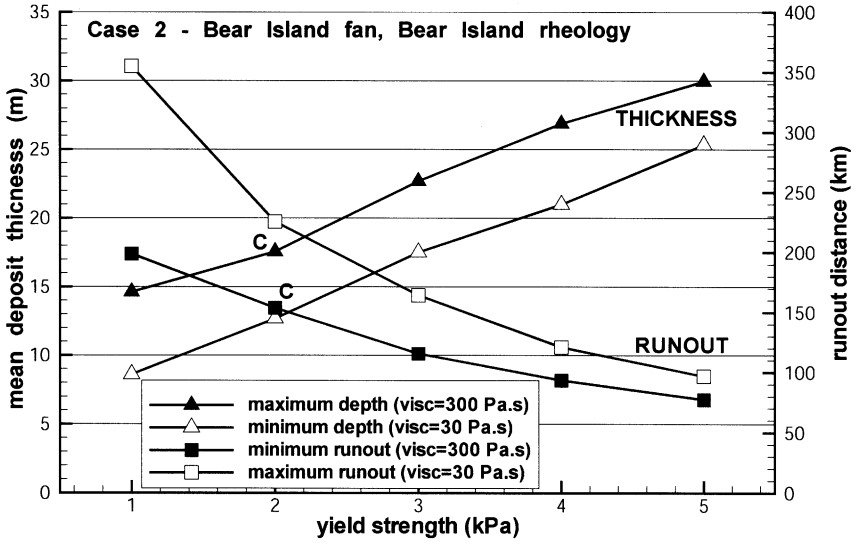

Fig. 7. Data plots from Case 2 simulations of the sediment flows on the Bear Island fan showing sediment runout and depth as a function of sediment yield. In this case yield strength is back-calculated from observed deposit depths on the Bear Island fan and Eq. 2 given in the text.

dramatic at low yield strength. Viscosity also shows a more dramatic effect on deposit thickness in Case 2 than in Case 1. This is most likely a result of the larger volume of sediment considered in Case 2.

Table 3 compares these results with those observed in the field. For the most part the simulation results fall within the data obtained from the field, especially for yield strengths between 2 and 4 kPa. Again, it is not surprising that the model results match those measured in the field since the yield strength values used in the model were computed from thickness and slopes observed in the field. The results verify that BING is able to reproduce field observations.

5.3. Case 3 – Bear Island fan simulation: visco-plastic, Isfjorden rheology

In this final case we assume the observed deposits on the Bear Island fan were influenced by additional flow mechanics other than just visco-plastic flow (i.e. hydroplaning). With this assumption, it is no longer reasonable to assume that the observed final deposit thickness of the debris flows is representative of the sediment yield strength. For example, the deposit thickness of laboratory subaqueous debris flows that hydroplane are often thinner than predicted by a Bingham model since the acceleration of the hydroplaning head acts to elongate the deposit (Mohrig et al., 1999; Marr et al., 2001). For this reason, sediment yield strength must be determined by a means other than final deposit thickness. Here, we make a simple assumption that the Bear Island sediment is rheologically similar to the sediment on the Isfjorden fan. This is a reasonable assumption since sediment source and composition are similar (Table 1). A potential caveat to this assumption is the influence of accumulation rates and in-situ water contents of the sediment on the rheological properties of the sediment. Implicit in Case 3 is the assumption that accumulation rate is similar in both regions. It is also important to emphasise that the version of BING used here is not capable of simulating hydroplaning dynamics. Rather, the simulations of Case 3 are of visco-plastic flows just as in Case 1 and 2, but the sediment yield strength is estimated from Isfjorden sediments rather than final deposit thickness.

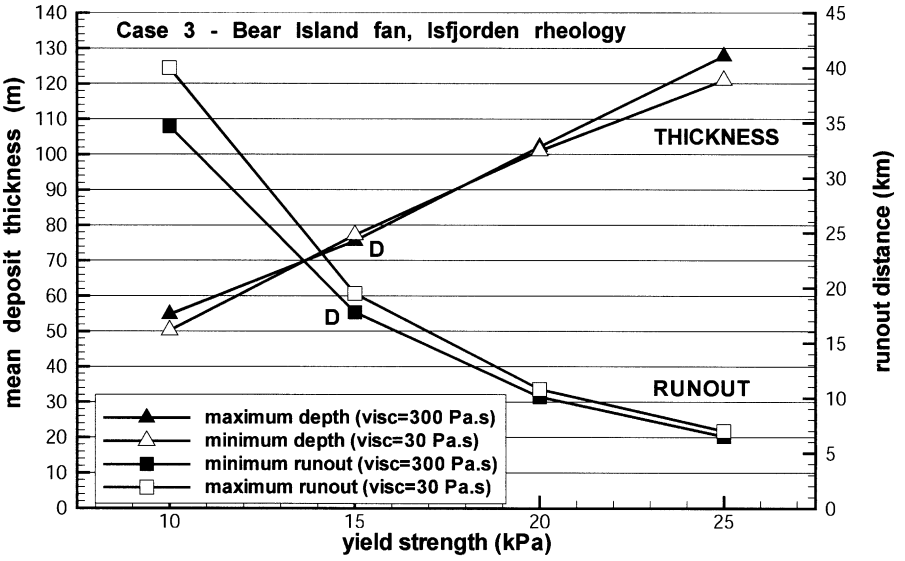

Fig. 8. Data plots from Case 3 simulations of the sediment flows on the Bear Island fan showing sediment runout and depth as a function of sediment yield. In this case we assume that additional flow dynamics took place during the event causing Eq. 2 to be invalid for calculating yield strength. Therefore, the yield strengths used in simulation are the same as those used for the Isfjorden fan simulations.

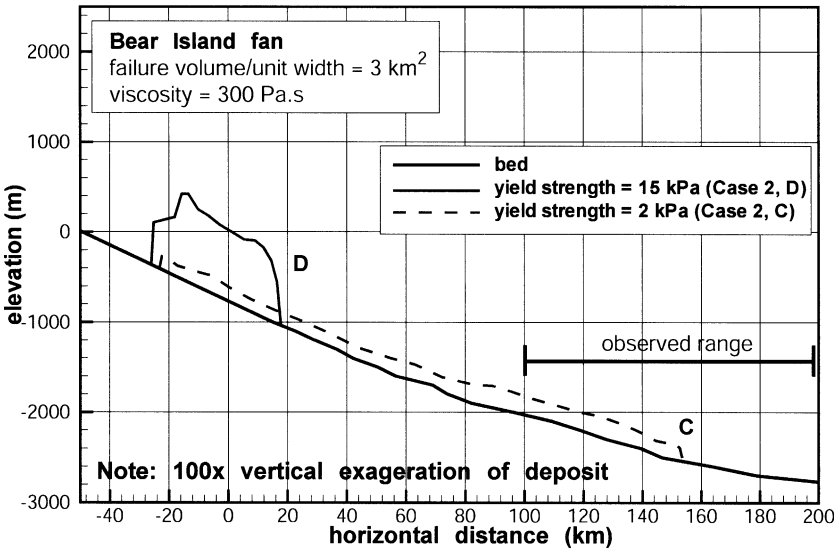

Fig. 9. Comparison plot of debris flow final geometry simulated by BING. The run with the large yield strength had a long runout distance (C) and the run with the low yield strength had a short runout distance (D). C and D are referenced in Figs. 7 and 8, respectively. There is a 100× vertical exaggeration of the deposit thicknesses.

Fig. 8 shows the results from the simulations. The combination of high yield strength and low slope resulted in very low runout distances and thick deposits. Variations in viscosity had little affect on deposit thickness or runout distance. Table 3 compares the results to the field observations. As expected the visco-plastic flow simulations fail to match the observations from the field with reasonable input parameter values.

6. Implications of results

The three cases described above reveal the parameters that are important in governing runout distance and thickness of subaqueous debris flow deposits. These parameters are described below.

Failure volume is more or less proportional to final runout distance on a given slope (Edgers and Karlsrud, 1982). Simulations not reported here show this to be true. Bear Island failure volumes were larger than Isfjorden failures, suggesting that failure volume may be a partial explanation for the longer runout. However, the simulations from cases 2 and 3 show that either a different rheology (lower yield strength) or a variation in flow mechanics (hydroplaning) along with the increase in volume are necessary to achieve the observed runout distances. Failure volume alone does not justify the difference. In other words, the Case 3 shows that if the Isfjorden and Bear Island debris flows have the same sediment properties, the difference in failure volumes alone is not enough to explain the differences in observed runout.

Increases in *yield strength* result in shorter runout distances and thicker final deposits. This is illustrated in Fig. 9 in which the results from the 2 kPa simulation in Case 2 (C) and the 15 kPa simulation in Case 3 (D), both with viscosity of 300 Pa s, are compared. In Case 3 the runout distance was very short, requiring an additional mechanism to generate the 100–200 km runout distances observed in the field.

The *dynamic viscosity* of the debris flow influences the runout most strongly in sediment with low yield strength (Case 2). In sediment with high yield strength (10–25 kPa), variations in viscosity have little affect on runout. The general trend is for low viscosity sediment to flow farther than high viscosity sediment.

7. Discussion and concluding remarks

The numerical model BING, describing the flow as a visco-plastic Bingham fluid, is used to investigate how sediment rheology and flow mechanics can possibly explain the variations in debris flow runout distances observed on the Isfjorden and Bear Island fans. The modelling revealed that several parameters influence final deposit runout and thickness. The longitudinal path profile, failure volume, yield strength, and dynamic viscosity all played a role in flow and deposition. Yield strength seemed to be the most important parameter in determining runout distance, while viscosity affected runout and thickness to a lesser extent. Bed slope and failure volume were easily measurable parameters while yield strength and viscosity are more difficult to measure and were therefore estimated. Sediment density is also an important parameter, however it was not investigated in depth in this study.

The large runout distances of the debris lobes on the Bear Island fan can be attributed either to a more fluidal sediment rheology or variation in the operating flow mechanics. In the former case, visco-plastic sediment with yield strengths of 2–4 kPa had runout distances of 100–200 km. In the latter case, high yield strength sediment (10–25 kPa) only flowed 10–35 km. Hence, a visco-plastic flow description fails with high yield strength sediment, and an additional mechanism such as hydroplaning is required to reach the 100–200 km observed in the field.

In recent laboratory-generated subaqueous debris flows, hydroplaning was observed to increase runout distance (Mohrig et al., 1998, 1999). Fig. 10 shows deposit thickness data from two experiments reported in Mohrig et al. (1999) as well as simulations of these experiments using BING. Run 3a was a subaerial run and Run 3w was a subaqueous run. Approximately 30 l of slurry was introduced into a 20-cm-wide channel. The confined channel was sloped at 6° from 0 to 5.7 m and at 1° from 5.7 to 10 m. The grain-size distribution of the slurry was chosen to model the composition of the debris flow sediment found on the Bear Island Fan. The slurry used in runs 3a and 3w had a measured yield strength of 36 Pa and a viscosity of 0.023 Pa s. For further details of the experiments see Mohrig et al. (1999).

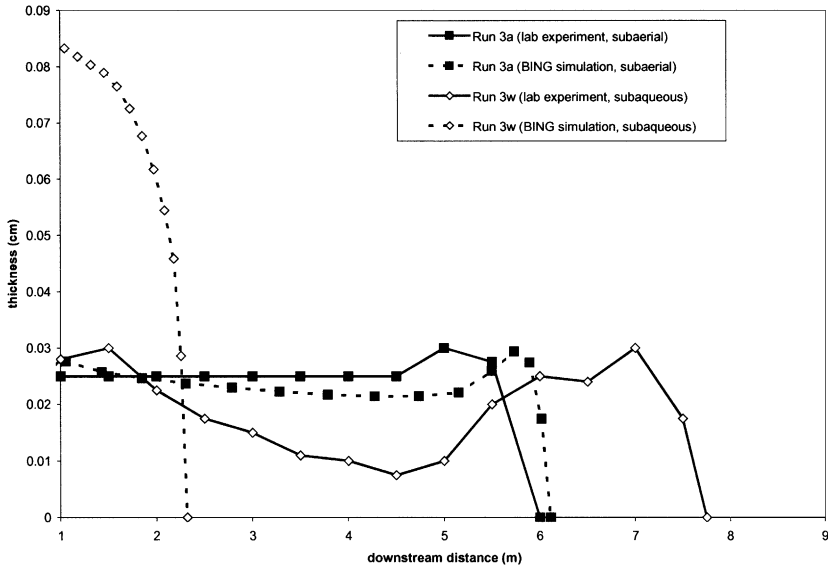

Fig. 10. Comparison of final deposit thickness for subaerial and subaqueous simulated (BING) and laboratory-generated debris flows. The results of the laboratory experiments are runs 3a and 3w presented in Mohrig et al. (1999). The simulation matches well the results of the lab experiment for the subaerial case but fails to reproduce the subaqueous case. The difference between simulation and experiment for the subaqueous case is do to hydroplaning of the laboratory flow (Run 3w).

Using BING to simulate subaerial Run 3a it was possible to generate a deposit similar to the experiment (Fig. 10), however it was necessary to use a sediment yield strength of 70 Pa rather than the reported 36 Pa. One possible reason for the need to artificially increase the yield strength was the influence of the confining walls on the physical experiments. BING is not able to capture lateral shearing of the slurry resulting from the confining walls of the experiment flume and thus may over-predict runout distances. Simulation of the same slurry run subaqueously, also with a τ_y of 70 Pa (Run 3w), shows a large discrepancy in the runout distances of the numerical and experimental debris flows. The difference can be attributed to the fact that the laboratory-generated debris flow in Run 3w hydroplaned allowing the slurry to run-out much farther than was predicted by a purely Bingham flow as seen in the results from the BING simulation (Fig. 10). It is possible that the same hydroplaning mechanism observed in the laboratory also influenced the runout of the submarine debris flow deposits found on the Bear Island fan.

The rheological parameters of the sediment (i.e. dynamic viscosity and yield strength) that strongly influence debris flow runout distance are also the parameters that are the most difficult to measure. Development of better techniques for measuring or estimating the rheological parameters of mud-rich debris flows is required before truly accurate numerical simulation of fine-grained subaqueous debris flows can be achieved.

Acknowledgements

Funding for this research was provided by EU program ENAM II (MAS3-CT95–003) and the Seabed/Norsk Hydro project. The authors thank Dieter Issler and Gary Parker for their support and review of this work. We would also like to thank Lincoln Pratson and two anonymous reviewers for their constructive reviews of this manuscript. A free copy of the numerical model BING can be obtained from the St. Anthony Falls Laboratory web site: www.umn.edu/safl.

References

Bagnold, R.A., 1954. Experiments on a gravity free dispersion of large solid spheres in a Newtonian fluid under shear. Proc. R. Soc. London Ser. A 225, 49–63.

Bagnold, R.A., 1956. The flow of cohesionless grains in fluids. Philos. Trans. R. Soc. London 249, 235–297.

Bea, R.G., 1971. How sea floor slides affect offshore structures. Oil Gas J. 69, 88–91.

Bjerrum, L., 1971. Subaqueous slope failures in Norwegian Fjords. Nor. Geotech. Inst. Publ. 88.

Coussot, P., 1997. Mudflow Rheology and Dynamics. Balkema, Rotterdam.

Dimakis, P., Elverhøi, A., Høeg, K., Solheim, A., Harbitz, C., Laber, T., Vorren, T., Marr, J., 2000. Submarine slope stability on high-latitude glaciated Svalbard-Barents Sea margins. Mar. Geol. 162, 303–316.

Dowdeswell, J.A., Siegert, M.J., 1999. Ice-sheet numerical modeling and marine geophysical measurements of glacier-derived sedimentation on the Eurasian Arctic continental margins. Geol. Soc. Am. Bull. 111, 1080–1097.

Edgers, L., Karlsrud, K., 1982. Soil flows generated by submarine slides – case studies and consequences. Nor. Geotech. Inst. Publ. 143.

Elverhøi, A., Norem, H., Andersen, E.S., Dowdeswell, J.A., Fossen, I., Haflidason, H., Kenyon, N.H., Laberg, J.S., King, E.L., Sejrup, H.P., Solheim, A., Vorren, T., 1997. On the origin and flow behaviour of submarine slides on deep-sea fans along the Norwegian-Barents Sea continental margin. Geo-Mar. Lett. 17, 119–125.

Hampton, M.A., 1975. Competence of fine-grained debris flows. J. Sediment. Petrol. 45, 834–844.

Hampton, M.A., Lee, H.J., Locat, J., 1996. Submarine landslides. Rev. Geophys. 34, 33–59.

Harbitz, C.B., 1992. Model simulations of tsunamis generated by the Storegga Slides. Mar. Geol. 105, 1–21.

Harbitz, C.B., Issler, D., Keylock, C.J., 1998. Conclusions from a recent survey of avalanche computational models. Nor. Geotech. Inst. Publ. 203, 25 Years of Snow Avalanche Research at NGI. Proc. Anniversary Conf. Voss, 12–16 May, 1998. Norwegian Geotechnical Institute, Oslo.

Harbitz, C.B., Parker, G., Elverhøi, A., Marr, J., Mohrig, D., Harff, P., in review. Hydroplaning of subaqueous debris flows and glide blocks: Analytical solutions and discussion. J. Geophys. Res., submitted.

Heezen, B.C., Ewing, M., 1952. Turbidity currents and submarine slumps, and the 1929 Grand Banks earthquake. Am. J. Sci. 250, 849–873.

Heim, A., 1932. Bergsturz und Menschenleben. Beiblatt zur Vierteljahresschrift der Natf. Ges. Zürich 20. Fretz und Wasmuth, Zurich, 218 pp. (English translation by Skermer, N., BiTech Publishers, Vancouver, 195 pp.).

Huang, X., García, M.H., 1998. A Herschel-Bulkley model for mud flow down a slope. J. Fluid Mech. 374, 305–333.

Huang, X., García, M.H., 1999. Modelling of non-hydroplaning mudflows on continental slopes. Mar. Geol. 154, 131–142.

Imran, J., Harff, P., Parker, G., 2001. A numerical model of submarine debris flow with graphical user interface. Comput. Geosci. 27, 721–733.

Iverson, R., 1997. The physics of debris flows. Rev. Geophys. 35, 245–296.

Jiang, L., LeBlond, P., 1993. Numerical modeling of an underwater Bingham plastic mudslide and the waves which it generates. J. Geophys. Res. 98 (C6), 303–310, 317.

Johnson, A.M., 1970. Physical Processes in Geology. Freeman, Cooper, San Francisco, CA, 577 pp.

Krause, D.C., White, W.C., Piper, D.J.W., Heezen, B.C., 1970. Turbidity currents and cable breaks in the western New Britain Trench. Geol. Soc. Am. Bull. 81, 2153–2160.

Kulikov, E.A., Rabinovich, A.B., Thomson, R.E., Bornhold, B.D., 1996. The landslide tsunami of November 3, 1994, Skagway Harbor, Alaska. J. Geophys. Res. 101, 6609–6615.

Laberg, J.S., Vorren, T.O., 1993. A late Pleistocene submarine slide on the Bear Island Trough Mouth Fan. Geo-Mar. Lett. 13, 227–234.

Laberg, J.S., Vorren, T.O., 1995. Late Weichselian debris flow deposits on the Bear Island Trough Mouth Fan. Mar. Geol. 127, 45–72.

Lee, H.J., 1989. Undersea landslides: extent and significance in the Pacific Ocean. In: Brabb, E.E. (Ed.), Landslides. Proc. 28th IGC Symposium, Washington DC. Elsevier, Amsterdam, pp. 367–379.

Lied, K., Bakkehøi, S., 1980. Empirical calculations of snow-avalanche run-out distance based on topographic parametres. J. Glaciol. 26, 165–177.

Locat, J., 1997. Normalized rheological behaviour of fine muds and their flow properties in a pseudoplastic regime. In: Chen, Cheng-lung (Ed.), First International Conf. on Debris Flow Hazards Mitigation: Mechanics, Prediction, and Assessment. San Francisco, CA, 7–9 August 1997.

Major, J.J., Pierson, T.C., 1992. Debris flow rheology: Experimental analysis of fine-grained slurries. Water Resour. Res. 28, 841–857.

Marr, J.G., Harff, P.A., Shanmugam, G., Parker, G., 2001. Experiments on subaqueous sandy gravity flows: The role of clay and water content in flow dynamics and depositional structures. Geol. Soc. Am. Bull. 113, 1377–1386.

McClung, D.M., Schaerer, P.A., 1993. The Avalanche Handbook. The Mountaineers, Seattle, WA, 265 pp.

Middleton, G.V., Hampton, M.A., 1973. Sediment gravity flows: Mechanics of flow and deposition. In: Middleton, G.V., Bouma, A.H. (Eds.), Turbidites and Deep-water Sedimentation: Pacific Section. Soc. Econ. Paleontol. Mineral., Los Angeles, CA, pp. 1–38.

Mohrig, D., Whipple, K.X., Hondzo, N.H., Ellis, C., Parker, G., 1998. Hydroplaning of subaqueous debris flows. Geol. Soc. Am. Bull. 110, 387–394.

Mohrig, D., Elverhøi, A., Parker, G., 1999. Experiments on the relative mobility of muddy subaqueous and subaerial debris flow, and their capacity to remobilize antecedent deposits. Mar. Geol. 154, 117–129.

Moore, D.G., 1978. Submarine slides. In: Voight, B. (Ed.), Rockslides and Avalanches, Vol. 1. Elsevier, Amsterdam, pp. 563–604.

Moore, G.W., Moore, J.G., 1988. Large-scale bedforms in boulder gravel produced by giant waves in Hawaii. Spec. Pap. Geol. Soc. Am. 229, 101–110.

Moore, J.G., Moore, G.W., 1984. Deposit from a giant wave on the island of Lanai. Science 226, 1312–1315.

Murty, T.S., 1979. Submarine slide-generated water waves in Kitimat Inlet, British Columbia. J. Geophys. Res. 84, 7777–7779.

Norem, H., Locat, J., Schieldrop, B., 1990. An approach to the physics and the modeling of submarine flowslides. Mar. Geotechnol. 9, 93–111.

O'Brien, J.S., Julien, P.Y., 1988. Laboratory analysis of mudflow properties. J. Hydraul. Eng. 114, 877–887.

Phillips, C.J., Davies, T.R., 1990. Determining rheological parameters of debris flow material. Geomorphology 4, 101–110.

Piper, D.J., Pirmez, C., Manley, P.L., Long, D., Flood, R., Normark, W.R., Showers, W., 1997. Mass transport deposits of the Amazon Fan. In: Flood, R.D., Piper, D.J.W., Klaus, A., Peterson, L.C. (Eds.), Proc. ODP Sci. Results 155, pp. 109–146.

Prior, D., Bornhold, B.D., 1986. Sediment transport on subaqueous fan delta slopes, Britannia Beach, British Columbia. Geo-Mar. Lett. 5, 217–224.

Salm, B., Burkard, A., Gubler, H.U., 1990. Berechnung von Fliesslawinen; eine Anleitung für Praktiker mit Beispielen. Mitteilungen des Eidgenössischen Institutes für Schnee- und Lawinenforschung 47.

Scheidegger, A.E., 1973. On the prediction of the reach and velocity of catastrophic landslides. Rock Mech. 5, 231–236.

Takahashi, T., 1978. Mechanical characteristics of debris flow. J. Hydraul. Div. Am. Soc. Civ. Eng. 104, 1153–1169.

Whipple, K.X., 1997. Open-channel flow of Bingham fluids: application in debris-flow research. J. Geol. 105, 243–262.